Immobilization of naringinase on asymmetric organic membranes: application for debittering of grapefruit juice

Yaiza González-Temiño, María O. Ruíz, Natividad Ortega, Sonia Ramos-Gómez and María D. Busto*

Department of Biotechnology and Food Science, Science Faculty, University of Burgos, Misael Bañuelos s/n, 09001 Burgos, Spain

***Corresponding author:** Faculty of Science, University of Burgos, Misael Bañuelos s/n, 09001 Burgos, Spain

E-mail addresses: dbusto@ubu.es (M.D. Busto)

ygonzalez@ubu.es (Y. González-Temiño); moruiz@ubu.es (M.O. Ruíz), nortega@ubu.es (N. Ortega), soniarg@ubu.es (S. Ramos-Gómez),

Abstract

An enzymatic membrane reactor (EMR) was performed by immobilizing naringinase onto polyethersulfone ultrafiltration membrane based on fouling-induced method. The effect of molecular weight cut-off and configuration of the membrane, applied pressure, enzyme concentration and pH were studied in terms of permeate rate, immobilization efficiency and biocatalytic conversion. The 10 kDa membrane operating in reverse mode, 0.2 MPa, 0.3 gL^{-1} of enzyme in acetate buffer at pH 5 and cross-linking with 0.25% glutaraldehyde showed the highest naringin conversion (73%). It was determined that the intermediate pore blocking model was the predominant fouling mechanism for the enzyme immobilization. The EMR was applied for debittering of grapefruit juice, achieving a conversion of naringin below bitterness threshold and maintaining the antioxidant capacity of the juice. Furthermore, the biocatalytic activity of immobilized enzyme was retained at a high level at least during three consecutive reaction runs, and with storage at 4 ºC overnight after each run.

Industrial relevance. The potential of membrane technologies in the juice industries is widely recognized today. The development of EMR with naringinase activity is an attractive option to traditional techniques for reducing bitterness due to its high specificity and effectiveness, possibility of repeated and continuous use, and in order to retain the properties of juice as much as possible. The research carried out represents an advance in the application of biocatalytic membranes as technological alternative for juice debittering.

Key words: enzymatic membrane reactor, naringinase, polyethersulfone membrane, crosslinking, debittering, grapefruit juice

1. Introduction

Consumers' interest in citrus juices has grown in the last years mainly due to its content in bioactive components (vitamin C, phenolic compounds…) that are beneficial for human health (Huang, Zhan, Shi, Chen, Deng, & Du, 2017). Nevertheless, fresh grapefruit juice also contains bitter flavanone glycosides, mainly naringin, which seriously compromises the quality and acceptability of these juices (Wang, Wang, Wu, & Shyu, 2018; Zhang, Ru, Jiang, Yang, Weng, & Xiao, 2020). Different techniques have been reported for debittering citrus juices, including adsorption and chemical methods. However, these technologies have some drawbacks affecting acidity, sweetness, flavour and turbidity of the juice, as well as poor efficiency (Huang et al., 2017). Enzyme treatment is a promising alternative to traditional techniques for reducing bitterness due to its high specificity and effectiveness. Naringinase is an enzymatic complex with α-L-rhamnosidase (EC 3.2.1.4) and β-D-glucosidase (EC 3.2.1.21) activities. First, α-L-rhamnosidase hydrolyses naringin into rhamnose and prunin (decreasing bitterness by two-thirds) and then, β-D-glucosidase converts prunin to glucose and naringenin (tasteless) (Zhang et al., 2020). The metabolite of naringin, naringenine, has showed antioxidant capacity and effectiveness in the protection against oxidative damage to lipids and DNA (Cavia-Saiz, Muñiz, Ortega, & Busto, 2011). Therefore, the treatment with naringinase for debittering of grapefruit juice would maintain its healthy properties (Ribeiro & Ribeiro, 2008).

The use of free naringinase involves different practical problems, including enzyme inhibition by acid pH and juice components (Norouzian, Hosseinzadeh, Inanlou, & Moazami, 2000), separation of the biocatalyst from the solution, low productivity, and high production costs. Enzyme immobilization technology can be used to solve these problems since enhances enzyme stability, allows its repeated and continuous use, and prevents the contamination of the final product (Busto, Cavia-Saiz, Ortega, & Muñiz, 2014; Sigurdardóttir

et al., 2018). However, the naringinase immobilization methods described so far (Luo et al., 2019; Mishra & Kar, 2003) have not been effective enough for its industrial application.

The potential of membrane technologies in the food and beverage processing is widely recognized today (di Corcia, Dhuique-Mayer, & Dornier, 2020; Sitanggang, Sumitra, & Budijanto, 2021). Membranes are also interesting supports for enzyme immobilization as they act as selective barrier which facilitates the separation of the biocatalyst from the product of reaction and provides high surface area for enzyme loading (Chakraborty et al., 2016; Sigurdardóttir et al., 2018). Furthermore, enzymatic membrane reactors (EMR) are especially useful in reactions in which product inhibition can occur (Cen, Liu, Xue, & Zheng, 2019). Rhamnose inhibits naringinase activity, making immobilization with membranes an interesting option. Different techniques can be used to immobilize enzymes in/on membranes: entrapment, adsorption, cross-linking or covalent attachment. One of the simplest immobilization strategies, called fouling induced method, is based on enzyme entrapment or adsorption in the membrane by deliberate promotion of fouling via pressure-driven filtration (Luo, Meyer, Jonsson, & Pinelo, 2014b). Fouling is influenced by the membrane properties, as the pore size and configuration, the process parameters, as applied pressure, and the feed conditions, as concentration and pH (Lim & Mohammad, 2010; Luo et al., 2014a; Luo et al., 2014b; She, Tang, Wang, & Zhang, 2009; Wang et al., 2018). These parameters must be studied to achieve maximum irreversible fouling and, consequently, more effective enzyme immobilization.

Immobilization by fouling induced technique involves physical interactions between the membrane and the enzyme, mainly Van der Waals forces, hydrogen bonds and electrostatic forces. Since weak bonds are established with the carrier, the biocatalyst can be released by a simple washing step or during reaction cycles (Cen et al., 2019). In order to reduce the possibility of desorption, enzyme molecules immobilized on the membrane can be further

cross-linked with a functional reagent such as glutaraldehyde (Yujun, Jian, Guangsheng, & Youyuan, 2008).

In the current study, immobilization of naringinase on ultrafiltration membranes by fouling induced method is investigated. Pore size and configuration of the membrane were studied as well as applied pressure, enzyme concentration and immobilization pH. In order to improve the stability of immobilization, further cross-linking with glutaraldehyde was implemented. The enzymatic membrane reactor was then used for debittering of grapefruit juice, and its catalytic efficiency and operational stability were determined. Finally, physicochemical characteristics and antioxidant activity of the treated juice were also analysed.

2. Material and Methods

2.1. Chemicals and Materials

Naringinase from *Penicillium decumbens* (CAS Number 9068-31-9), naringin and glutaraldehyde (grade II) were purchased from Sigma Chemical Co. (St Louis, MO, USA). All other reagents were of analytical grade.

10 and 30 kDa polyolefin-supported polyethersulfone asymmetric ultrafiltration membranes (Biomax10 and Biomax30 from Millipore, USA) with an effective surface area of 13.4 cm^2 were used.

2.2. Preparation of enzymatic membrane reactors

Immobilization was performed in a 50 mL stirred cell (Amicon 8050, Millipore, USA) with the membrane placed at the bottom. This cell was equipped with a gas inlet which allows to keep constant transmembrane pressure (ΔP). Permeate fluxes (J_p) were determined with volumetric cylinders and gravimetrically throughout experiment. All experiments were carried out at least twice in order to verify the reproducibility of the results, and a new membrane was used each time.

111 Biomax membranes were first cleaned by filtering 150 ml of Mili-Q water at 0.35 MPa
112 (procedure according to the manufacturers' instructions). Afterwards, intrinsic membrane
113 permeability was measured at different pressures (0.05-0.3 MPa) with the same buffer used
114 for enzyme immobilization.
115 Naringinase was immobilized by the fouling-induced technique previously described by
116 Luo et al. (2014a) with some modifications; 30 mL of enzyme solution were filtered applying
117 pressure by filling nitrogen gas into the filtration cell, at room temperature and constant
118 stirring of 100 rpm. Permeate was collected every 4 mL to a final volume of 28 mL. At the
119 end of filtration, the fouled membrane was rinsed 3 times with immobilization buffer (5 mL
120 each time) without applying any pressure, and the rising residual was mixed with the
121 retentate (2 mL). After that, the membrane was washed with 100 mL of immobilization buffer
122 at a pressure of 0.2 MPa.
123 The effect of membrane pore size, 10 and 30 kDa, and membrane configuration, normal
124 (skin material toward feed) and reverse (support material toward feed) mode, were studied.
125 Different pressures (0.1, 0.2 and 0.3 MPa), enzyme concentrations (0.2, 0.3 and 0.4 g L^{-1})
126 and pH (3, 5 and 7) were also tested. Enzyme immobilized by fouling-induced onto the
127 asymmetric membrane was further cross-linked with glutaraldehyde (Yujun et al., 2008).
128 Glutaraldehyde solution (20 mL) at different concentrations (0.10, 0.25, 0.50 and 1.0% (v/v))
129 was filtered through the fouled membrane under a pressure of 0.15 MPa and stirring of 100
130 rpm. Afterwards, the membrane was rinsed twice with 0.2 M acetate buffer at pH 5 (30 mL
131 each time), 0.2 MPa and 100 rpm.

132 *2.2.1. Calculated parameters*

133 The amount of immobilized enzyme was calculated from the following mass balance:

$$m_i = C_f V_f - C_p V_p - C_r V_r - C_w V_w \quad (1)$$

134 where m_i is the immobilized enzyme amount; C_f is the enzyme concentration in the feed, C_p
135 is the enzyme concentration in the permeate, C_r is the enzyme concentration in the mixture

136 of retentate and rising residual, and C_w is the enzyme concentration in the pressured
137 washing permeates. V_f, V_p, V_r and V_w are the volumes in the feed solution, permeate, in the
138 mixture of retentate and rising residual, and in the washing with pressure, respectively.

139 The enzyme concentration was measured by Bradford protein assay (Bradford, 1976).
140 5 mL of Bradford reagent was added to 0.5 mL of sample and the colour developed was
141 determined spectrophotometrically at 595 nm. A standard curve of naringinase in the range
142 of 0-0.5 g L^{-1} was plotted. All samples were measured in triplicate.

143 The immobilization efficiency (IE) was calculated as follows:

$$IE\ (\%) = \frac{m_i}{m_t} \times 100 \quad (2)$$

144 where m_t is the amount of total enzyme (in the feed) and m_i is the amount of immobilized
145 enzyme.

146 Considering a resistance-in-series model, the total resistance of the membrane, R_t (m^{-1}
147 ^{1}), can be written as:

$$R_t = \frac{1}{\mu \cdot Lp} = R_m + R_{cp} + R_{rf} + R_{if} \quad (3)$$

148 where, μ is the solvent viscosity (Pa s), Lp is the membrane permeability (m s^{-1} Pa^{-1}), R_m is
149 the membrane hydraulic resistance (m^{-1}), R_{cp} is the resistance due to concentration
150 polarization effects (m^{-1}), R_{rf} is the resistance resulting from reversible fouling (m^{-1}) and R_{if}
151 is the irreversible fouling resistance (m^{-1}). Irreversible fouling capacity can be considered as
152 the most desirable effect in the enzyme immobilization process in order to avoid enzyme
153 losses during EMR reuses.

154 Different filtration resistances were calculated as follows: R_m was calculated from the
155 permeability of the buffer before enzyme immobilization; R_t could be determined from the
156 permeate flux at the end of immobilization; the sum of R_m, R_{rf} and R_{if} was obtained from the
157 permeability of the buffer at the beginning of the washing step with pressure, due to the
158 concentration polarization layer was removed by the rising without pressure ($R_{cp} = R_t - R_m -$

159 R_{rf} - R_{if}); and the sum of R_m and R_{if} was determined from the buffer permeability at the end
160 of the pressured washing step since reversible fouling was wiped off by the washing with
161 pressure and agitation.

162 *2.2.2. Membrane fouling model*

163 The type of membrane fouling, during naringinase immobilization, was investigated
164 using the Hermia's model (Hermia, 1982). This model was developed for a dead-end
165 filtration at a constant pressure and can be described as:

$$\frac{d^2t}{dV^2} = K\left(\frac{dt}{dV}\right)^n \quad (4)$$

166 where *t* is filtration time (s), *V* is permeate volume (L), *K* is the constant and *n* can take
167 different values depending on different types of fouling: *n*=2 indicates the complete blocking
168 model, *n*=1.5 for the standard blocking model, *n*=1 represents the intermediate blocking
169 model, and *n*=0 for the cake layer model. When *n* is fixed, four linear expressions can be
170 obtained by integrating Eq. (4):

when n=2, $$\ln J_p = \ln J_o - K_c t \quad (5)$$

when n=1.5, $$\frac{1}{J_p^{0.5}} = \frac{1}{J_o^{0.5}} + K_s t \quad (6)$$

when n=1, $$\frac{1}{J_p} = \frac{1}{J_o} + K_i t \quad (7)$$

when n=0, $$\frac{1}{J_p^2} = \frac{1}{J_o^2} + K_{cl} t \quad (8)$$

171 where J_p is the permeate flux, J_o is the certain permeate flux a t=0, and K_c, K_s, K_i, K_{cl} are the
172 constants for complete blocking, standard blocking, intermediate blocking and cake layer
173 models, respectively. The most possible fouling mechanism can be identified by fitting the
174 experimental flux data using these linear models and comparing their determination

coefficients, R^2 (Lamdande, Mittal, & Raghavarao, 2020; Luo, Meyer, Jonsson, & Pinelo, 2013).

177 *2.3. Enzymatic reaction*

178 To evaluate the activity of immobilized naringinase, 50 mL of substrate solution
179 (0.8 g L^{-1} of naringin in 0.2 M acetate buffer at pH 5) was charged into the stirred cell
180 equipped with the biocatalytic membrane. A pressure of 0.025 MPa was applied until 48 mL
181 of permeate was obtained, maintaining the temperature at 45-50 ºC and a constant stirring
182 of 100 rpm. Aliquots of 4 mL from permeate were separated and cooled on ice immediately
183 to stop the reaction. The retentate (2 mL) was also collected to check if there was reaction
184 in the bulk solution.

185 The substrate conversion was determined based on the quantification of the remaining
186 naringin in permeate using Davis' method (Davis, 1947). Aliquots of 0.1 mL of sample were
187 added to 0.1 mL of 4 M sodium hydroxide and 0.8 mL of diethylene glycol (90 %, v/v). The
188 assay mixture was allowed to stand for 15 min and the intensity of the yellow colour
189 developed was then read at 420 nm. The calibration line, in the range of 0-0.5 g L^{-1}, was
190 prepared from a standard solution of naringin. Samples were analyzed in triplicate.

191 *2.4. Grapefruit debittering by naringinase-membrane reactor*

192 Star Ruby grapefruits were purchased from a local supermarket and kept refrigerated
193 (4 ºC) until they were processed. Juice was obtained by using a domestic squeezer and the
194 seeds were removed with a strainer. Then, to avoid membrane collapse, the pulp was
195 removed by centrifugation (9000 rpm, 10 min) followed by vacuum filtration through a
196 fiberglass filter (APFC, 1.2 µm pore size) (Bhattacharjee, Saxena, & Dutta, 2017; Tsen, Tsai,
197 & Yu, 1989).

198 For debittering, 15 mL of clarified juice were poured into the stirred cell equipped with
199 the biocatalytic membrane followed by two other batches (10 mL each batch). The reaction
200 was carried out at 45-50 ºC, 0.025 MPa and 100 rpm. When 30 mL of permeate were
201 obtained, the filtration was stopped and the retentate (5 mL) was collected. Afterwards, the

membrane was rinsed with 30 mL of 0.2 M acetate buffer (pH 5) at room temperature applying a pressure of 0.2 MPa.

To study the operational stability of the EMR, the biocatalytic membrane was reused in three consecutive cycles and stored at 4 ºC overnight after each cycle. Before cycles, enzymatic membrane was preconditioned in 10 mL of acetate buffer (pH 5) for 15 min.

2.5. Grapefruit characterization

Fresh and debittered juice samples were analysed to determine naringin, pH, titratable acidity, soluble solids, and total antioxidant capacity.

The quantification of naringin in the juice samples was carried out by the method described by Davis (1947) (see section 2.3).

The pH and soluble solids content (ºBrix) were measured at 20 ºC using a digital pH-meter and a refractometer (Atago 3T), respectively. The total titratable acidity was assessed by titration with NaOH (0.05 M) and expressed as g of citric acid/L of grapefruit juice (Agencia Española de normalización y Certificación [AENOR], 1997).

The antioxidant capacity of juice samples was evaluated by ABTS method according to Rivero-Pérez, Muñiz and González-Sanjosé (2007). An amount of 40 µL of juice sample (at a dilution of 1:8) was mixed with 960 µL of the ABTS solution and completed to 1 mL with distilled water. After 15 min, the absorbance was measured at 734 nm. The results were expressed in mM Trolox equivalents, using a linear calibration obtained with different concentrations of Trolox (0-1.4 mM). Percentage inhibition was calculated as follows:

$$\text{Inhibition (\%)} = 1 - \frac{A_{sample}}{A_{control}} \quad (9)$$

where $A_{control}$ is the absorbance of ABTS solution in absence of sample and A_{sample} is the absorbance of ABTS radical solution mixed with juice sample. All determinations were performed in triplicate.

3. Results and discussion

3.1. Fouling-induced naringinase immobilization

3.1.1. Effect of membrane pore size and configuration

It is well known that both molecular weight cut-off (MWCO) and configuration have a great influence on membrane fouling (Prazeres & Cabral, 1994). In order to study the effect of these parameters on enzyme loading and activity, MWCO of 10 and 30 kDa, and reverse and normal mode configurations were investigated. For these experiments, a pressure of 0.2 MPa was fixed and an enzyme solution of 0.3 g L^{-1} in 0.2 M acetate buffer at pH 5 was filtered. As shown in Figure 1A, the increase in pore size resulted in higher initial permeate flux, whereas the flux at the end of filtration was almost the same due to membrane fouling. Experimental evidence suggested that initial permeate flux behaviour is highly dependent on membrane properties (pore size, materials, etc.) while final flux performance is controlled by fouling process (Luo et al., 2014b). Permeate flux behaviour during immobilization was also affected by membrane configuration (Figure 1A). The flux decreased by 96% for the reverse mode and 46% for normal mode, indicating that fouling increased when support layer was facing enzyme solution. Furthermore, from the analysis of filtration resistances (Figure 1A) it can be concluded that fouling increased (higher R_t) and enzyme immobilization was more stable (higher R_{if}) for Biomax 10 operating in reverse mode.

MWCO and configuration of the membrane also affected the immobilization efficiency. The increase in MWCO from 10 to 30 kDa resulted in a decrease in IE from 87.3 to 71.8%, respectively; probably because the larger pore size facilitated the passage of enzyme molecules through the membrane, appearing in the permeate (Table 1). Also, it is evident

247 that reverse configuration favoured membrane fouling, as the IE dramatically dropped from
248 87.3% to 16.7% for reverse and normal mode, respectively. The smaller pore size of the
249 skin layer hindered the deposition of the enzyme on the membrane and favoured its
250 rejection, remaining in the retentate (Table 1).

251 The enzymatic membranes were used to catalyse the hydrolysis of naringin in a buffered
252 solution at pH 5. The conversion achieved was 28.3 ± 3.5%, 4.5 ± 1.0% and 7.0 ± 1.5%,
253 with reaction times of 134, 28 and 36 min, using 10 kDa membranes in reverse and normal
254 mode, and 30 kDa membrane in reverse mode, respectively. The highest catalytic efficiency
255 obtained for 10 kDa membrane in reverse configuration could be attributed to the higher
256 amount of enzyme immobilized in/on the membrane and the longer operating time that
257 favoured the contact between the enzyme and substrate. Therefore, this MWCO and
258 reverse configuration were selected for the following experiences.

259 *3.1.2. Effect of transmembrane pressure*

260 In ultrafiltration processes the increase of transmembrane pressure (TMP) usually
261 promotes a more severe fouling because of higher drag force and enhancement of
262 concentration polarization (Wang & Tang, 2011). As shown in Figure 1B, the initial permeate
263 flux was higher with increasing of TMP. However, as the experiment progressed the flux
264 differences between the pressures were balanced as a consequence of fouling. Flux
265 reduction was 85.9%, 94.4%, and 95.3% for 0.1, 0.2 and 0.3 MPa, respectively; the
266 reduction was more moderate at 0.1 MPa because of lower total filtration resistance (Figure
267 1B).The increase in TMP from 0.1 MPa to 0.2 MPa favoured stable fouling, as can be seen
268 by the increase in R_{if} (Figure 1B). In contrast, concentration polarization appeared at 0.3
269 MPa which involved an increase in R_t without producing an effective immobilization of
270 naringinase. On the other hand, the amount of immobilized enzyme was similar for all the
271 pressures, obtaining an immobilization efficiency between 87 and 95% (Table 1).

272 Naringin conversion by the immobilized enzyme was 24.6 ± 1.7%, 24.5 ± 7.2% and 22.7

273 ± 3.0% for 0.1, 0.2 and 0.3 MPa, respectively. No significant differences were found in
274 catalytic capacity (ANOVA, p>0.05) which agrees with IE results.

275 Finally, the pressure of 0.2 MPa was selected for the subsequent experiments since the
276 irreversible filtration resistance was increased and concentration polarization was avoided.

277 *3.1.3. Effect of enzyme concentration and pH*

278 Membrane fouling is also influenced by the conditions of the feed, as enzyme
279 concentration. Usually, raising feed concentration accelerates fouling because the particles
280 are more likely to deposit or aggregate on the membrane or to block its pores (Luo et al.,
281 2014a). As feed concentration increased, permeate flux decreased further whereas total
282 and irreversible resistance increased (Figure 2A). These results are in agreement with those
283 obtained by Corbatón-Báguena, Gugliuzza, Cassano, Mazzei, and Giorno (2015) who
284 demonstrated that severe fouling was produced when increasing the protein concentration.
285 No significant differences were found on IE between concentrations (Table 2).

286 Regarding the data for naringin conversion, 24.5 ± 7.2%, 28.8 ± 3.5% and 35.4 ± 1.0%
287 for 0.2, 0.3 and 0.4 g L^{-1} of enzyme, respectively, the catalytic activity was higher for the
288 bioreactor prepared with a concentration of 0.4 g L^{-1}. Nevertheless, this concentration was
289 discarded because this increase in enzyme activity was not enough to compensate the long
290 operating time of 6.7 h.

291 Enzyme immobilization by fouling induced technique is expected to be influenced by the
292 pH solution as it affects the charge and hydrophilicity of both membrane and solutes of the
293 feed (Luo & Wan, 2013). Therefore, the effect of different pH values, 3, 5 and 6, was
294 analysed using Biomax 10 in reverse mode, and fixed conditions of 0.2 MPa and 0.3 g L^{-1}
295 of enzyme. Both acetate and citrate buffers were applied because acetate, used in the first
296 trials and to evaluate the enzyme activity, does not cover the pH range of study.

297 Different authors suggest that membrane fouling is higher at the isoelectric point of the
298 protein because the electrostatic repulsions between the molecules are at the minimum

299 which facilitates hydrophobic adsorption (Lim & Mohammad, 2010; Luo et al., 2014a; She
300 et al., 2009). Considering that the isoelectric point of naringinase is close to pH 5 (Ono,
301 Tosa, & Chibata, 1978), the results found in this study are in line with this hypothesis. When
302 the pH of the solution was 5, the permeate flux decreased more quickly and the R_{if} was
303 higher (Figure 2B), suggesting a severe and more stable fouling. When the pH moves away

304 from the isoelectric point, electrostatic repulsion between proteins raises, so membrane
305 fouling decreased (Lim & Mohammad, 2010). This would explain why total resistance was
306 lower at pH 3 (Figure 2B). The interaction between enzyme and membrane was weaker at
307 pH 6 as can be seen by the higher R_{rf} (Figure 2B) and the lower IE (Table 2). At pH above
308 the isoelectric point, the protein is negatively charged, so electrostatic repulsion between
309 molecules could limit adsorption to the membrane and also alter conformational structure
310 (Jones & O'Melia, 2000).

311 The catalytic capacity of EMR was also affected by the immobilization pH. Substrate
312 conversion was 20.4 ± 2.9%, 33.7 ± 2.7%, and 12.4 ± 1.7%, for pH 3, 5 and 6, respectively.
313 A higher conversion was achieved for pH 5, because the largest irreversible fouling
314 resistance (R_{if} in Figure 2B) improved the contact between naringinase and its substrate.
315 Naringin conversion was slightly lower, 28.8 ± 3.5%, when acetate buffer (pH 5) was used,
316 however, it was selected for naringinase immobilization due to citrate phosphate buffer
317 generated some turbidity that could compromise the operation of the EMR.

318 *3.2. Study of the fouling mechanism*

319 In order to study the fouling mechanism of membrane during naringinase immobilization,
320 four linear models (complete blocking, standard blocking, intermediate blocking and cake
321 layer) were utilized. For all the experiences described in section 3.1, the models were
322 calculated by fitting experimental flux data, and the most possible fouling mechanism was
323 founded by comparing the determination coefficients (R^2). According to Hermia's model, the
324 best fitting model was intermediate pore blocking model (R^2= 1.000). This type of fouling

implies that naringinase particles not only cause pore blocking, but also attach other particles on the membrane surface (Zheng et al., 2018). Although this type of fouling is less stable than complete or standard blocking, it could be the most effective mechanism for enzyme immobilization, since the pores of the membrane are not completely blocked and the passage of substrates and products could be facilitated, favouring catalytic activity.

3.3. Crosslinking with glutaraldehyde

One of the main limitations of fouling-inducd technique as immobilization strategy is the possibility of enzyme desorption during operating cycles. In order to enhance the stability of immobilization and EMR performance, enzyme molecules in the pores or in the membrane surface were cross-linked with glutaraldehyde based on the method described by Yujun et al. (2008). For this, naringinase was immobilized by induced fouling under the optimized conditions, Biomax 10 membrane operating in reverse mode, 0.2 MPa of pressure and 0.3 g L^{-1} enzyme in acetate buffer at pH 5. Afterwards, a glutaraldehyde solution at different concentrations, 0.10, 0.25, 0.50 and 1.0% (v/v), was filtered through the membrane to cross-link the enzymes.

As shown in Figure 3, after cross-linking with glutaraldehyde there was a significant increase in the performance of the enzyme membrane bioreactor. Without cross-linking, about 39.5% of immobilized naringinase was washed off during enzymatic reaction causing a quickly decline in naringin conversion. However, after cross-linking only 7.3% of naringinase was released during reaction, indicating the enzyme aggregates formed by cross-linking were more stable against the water wash (Yujun et al., 2008). The naringin conversion of the EMR without crosslinking was 28.8 ± 3.5%, while after cross-linking conversion increased to 59.4-73.3% depending on glutaraldehyde concentration. This improvement in catalytic behaviour of EMR has also been observed for the immobilization of lipases onto polysulfone membranes (Yujun et al., 2008; Zhu et al., 2016).

Based on the results shown in Figure 3, glutaraldehyde concentration of 0.25% was chosen as the optimal condition, since at 0.1% the conversion showed a downward trend and above 0.25% the hydrolysis of the substrate was not improved.

353 *3.4. Grapefruit debittering by the EMR*

354 Firstly, catalytic efficiency of the EMR for debittering was studied in synthetic juice (Gray
355 & Olson, 1981), with a composition of 0.8 g L^{-1} naringin, 47.5 g L^{-1} saccharose, 0.25 g L^{-1}
356 citric acid, and pH 3.2. The high conversion of naringin obtained with the synthetic juice,
357 76.8 ± 0.2%, suggests that the membrane and the crosslinking protect the enzyme against
358 the inhibitory effects of citric acid and the reaction products, rhamnose and glucose.

359 Naringin conversion with the EMR, operating with natural grapefruit juice, was 50.1±
360 0.3%. This decrease in catalytic activity of bioreactor could be the result of the acidic pH of
361 natural juice (2.9) and/or the presence of other enzyme inhibitors such as fructose or divalent
362 cations (Ca^{2+}, Mg^{2+} or Zn^{2+}) (Martearena, Daz, & Ellenrieder, 2008; Norouzian et al., 2000).
363 Nevertheless, enzymatic treatment reduced naringin content from 762 to 337 mg L^{-1}, below
364 bitterness threshold which is around 300-400 mg L^{-1} in grapefruit juice (Soares & Hotchkiss,
365 1998).

366 Operational stability of the EMR for debittering of grapefruit juice was also studied since
367 reusability of biocatalyst is of key importance for industrial application. As seen in Figure 4A
368 there was no apparent decrease in the conversion of the bitter compound during at least
369 three reaction cycles at 50 ºC. Furthermore, the biocatalytic membrane practically retained
370 its initial activity by storing it overnight at 4 ° C after each cycle. On the other hand, a slight
371 but progressive fouling of the membrane was observed, as evidenced by the decrease in
372 the permeate flux (Figure 4B).

373 The application of immobilized naringinase in ultrafiltration membranes for grapefruit
374 juice debittering has only been previously reported in two studies, Olson, Gray, & Guadagni
375 (1979) and Gray & Olson (1981). These authors developed a hollow fiber reactor with
376 naringinase from *Aspergillus niger* that reduced 67% of the naringin after recirculating the
377 juice several times at 45 ºC. However, there are no data of the operational stability of the
378 enzymatic reactor.

The effect of grapefruit juice debittering by the biocatalytic membrane on some physico-chemical characteristics of juice was also determined. The soluble solids content was not modified in the treated juice and, pH and titratable acidity were slightly affected, although these last parameters were close to those reported by other authors for fresh juice (Kola, Kaya, Duran, & Altan, 2010; La Cava & Sgroppo, 2015).

In order to study the effect on antioxidant capacity, ABTS assay was used. Treatment with the EMR showed minimal effect on the antioxidant capacity of juice, obtaining 3.69 ± 0.20 and 3.35 ± 0.04 mM Trolox for fresh and processed juice, respectively. Previous studies showed that the enzymatic treatment with free or immobilized naringinase improved total antioxidant capacity of grapefruit juice due to the increase in naringenin content (Cavia-Saiz et al., 2011). However, treatment for debittering of grapefruit or orange juice, with Amberlite IR-400 (Cavia-Saiz et al., 2011) or with Lewait VPOC 1064 (Stinco et al., 2013), respectively, caused losses around 25% of its antioxidant capacity.

4. Conclusions

Naringinase from *P. decumbens* was successfully immobilized onto polyethersulfone ultrafiltration membrane by fouling-induced technique and crosslinking with glutaraldehyde. The optimal results in naringin conversion (73%) were obtained with a membrane pore size of 10 kDa, in reverse mode configuration, transmembrane pressure of 0.2 MPa, 0.3 g L^{-1} of enzyme at pH 5, and crosslinking with 0.25% glutaraldehyde.

The EMR with immobilized naringinase was successively reutilized for debittering of grapefruit juice at least during three cycles at 50 ºC, achieving a reduction of 50% in the content of naringin, without modifying the pH, soluble solids content and titratable acidity, and with minimal reduction in the antioxidant capacity of juice. In order to avoid previous clarification of the juice, membrane operational design might be modified in future work. This research confirms the potential of biocatalytic membranes as a promising alternative for juice debittering.

References

Agencia Española de Normalización y Certificación [AENOR]. (1997). Zumos de frutas y hortalizas. Determinación de la acidez valorable. UNE-EN 12147.

Bhattacharjee, C., Saxena, V., & Dutta, S. (2017). Fruit juice processing using membrane technology: A review. *Innovative Food Science & Emerging Technologies*, *43*, 136–153. https://doi.org/10.1016/j.ifset.2017.08.002.

Bradford, M. M. (1976). A rapid and sensitive method for the quantitation of microgram quantities of protein utilizing the principle of protein-dye binding. *Analytical Biochemistry*, *72*(1), 248–254. https://doi.org/10.1016/0003-2697(76)90527-3.

Busto, M. D., Cavia-Saiz, M., Ortega, N., & Muñiz, P. (2014). Enzymatic debittering on antioxidant capacity of grapefruit juice. In V. Preedy (Ed.), *Processing and impact on antioxidants in beverages* (pp. 195–202). San Diego: Academic Press. https://doi.org/10.1016/B978-0-12-404738-9.00020-9.

Cavia-Saiz, M., Muñiz, P., Ortega, N., & Busto, M. D. (2011). Effect of enzymatic debittering on antioxidant capacity and protective role against oxidative stress of grapefruit juice in comparison with adsorption on exchange resin. *Food Chemistry*, *125*, 158–163. https://doi.org/10.1016/j.foodchem.2010.08.054.

Cen, Y. K., Liu, Y. X., Xue, Y. P., & Zheng, Y. G. (2019). Immobilization of enzymes in/on membranes and their applications. *Advanced Synthesis & Catalysis*, *361*(24), 5500–5515. https://doi.org/10.1002/adsc.201900439.

Chakraborty, S., Rusli, H., Nath, A., Sikder, J., Bhattacharjee, C., Curcio, S., & Drioli, E.

(2016). Immobilized biocatalytic process development and potential application in membrane separation: A review. *Critical Reviews in Biotechnology*, *36*(1), 43–48. https://doi.org/10.3109/07388551.2014.923373.

di Corcia, S., Dhuique-Mayer, C., & Dornier, M. (2020). Concentrates from citrus juice obtained by crosflow microfiltration: Guidance of the process considering carotenoid bioaccessibility. *Innovative Food Science and Emerging Technologies*, *66*, 102526. https://doi.org/10.1016/j.ifset.2020.102526.

Corbatón-Báguena, M. J., Gugliuzza, A., Cassano, A., Mazzei, R., & Giorno, L. (2015). Destabilization and removal of immobilized enzymes adsorbed onto polyethersulfone ultrafiltration membranes by salt solutions. *Journal of Membrane Science*, *486*, 207–214. https://doi.org/10.1016/j.memsci.2015.03.061.

Davis, W. B. (1947). Determination of flavanones in citrus fruits. *Analytical Chemistry*, *19*(7), 476–478. https://doi.org/10.1021/ac60007a016.

Gray, G. M., & Olson, A. C. (1981). Hydrolysis of high levels of naringin in grapefruit juice using a hollow fiber naringinase reactor. *Journal of Agricultural and Food Chemistry*, *29*(6), 1298–1301. https://doi.org/10.1021/jf00108a051.

Hermia, J. (1982). Constant pressure blocking filtration laws-application to power-law non-Newtonian fluids. *Transactions Institution of Chemical Engineers*, *60*(3), 183–187.

Huang, W., Zhan, Y., Shi, X., Chen, J., Deng, H., & Du, Y. (2017). Controllable immobilization of naringinase on electrospun cellulose acetate nanofibers and their application to juice debittering. *International Journal of Biological Macromolecules*, *98*, 630–636. https://doi.org/10.1016/j.ijbiomac.2017.02.018.

Jones, K. L., & O'Melia, C. R. (2000). Protein and humic acid adsorption onto hydrophilic membrane surfaces: Effects of pH and ionic strength. *Journal of Membrane Science*, *165*, 31–46. https://doi.org/10.1016/S0376-7388(99)00218-5.

Kola, O., Kaya, C., Duran, H., & Altan, A. (2010). Removal of limonin bitterness by treatment

457 of ion exchange and adsorbent resins. *Food Science and Biotechnology*, *19*(2), 411–
458 416. https://doi.org/10.1007/s10068-010-0058-2.
459 La Cava, E. L. M., & Sgroppo, S. C. (2015). Evolution during refrigerated storage of bioactive
460 compounds and quality characteristics of grapefruit [*Citrus paradisi* (Macf.)] juice
461 treated with UV-C light. *LWT - Food Science and Technology*, *63*(2), 1325–1333.
462 https://doi.org/10.1016/j.lwt.2015.04.013.
463 Lamdande, A. G., Mittal, R., & RAghavarao, K. S. M. S. (2020). Flux evalutation based on
464 fouling mechanism in acoustic field-assisted ultrafiltration for cold sterilizatin of tender
465 coconut water. *Innovative Food Science and Emerging Technologies, 61*, 102312.
466 https://doi.org/10.1016/j.ifset.2020.102312.
467 Lim, Y. P., & Mohammad, A. W. (2010). Effect of solution chemistry on flux decline during
468 high concentration protein ultrafiltration through a hydrophilic membrane. *Chemical*
469 *Engineering Journal*, *159*(1–3), 91–97. https://doi.org/10.1016/j.cej.2010.02.044.
470 Luo, J., Li, Q., Sun, X., Tian, J., Fei, X., Shi, F., Zhang, N., & Liu, X. (2019). The study of the
471 characteristics and hydrolysis properties of naringinase immobilized by porous silica
472 material. *RSC Advances*, *9*(8), 4514–4520. https://doi.org/10.1039/C9RA00075E.
473 Luo, J., Marpani, F., Brites, R., Frederiksen, L., Meyer, A. S., Jonsson, G., & Pinelo, M.
474 (2014a). Directing filtration to optimize enzyme immobilization in reactive membranes.
475 *Journal of Membrane Science*, *459*, 1–11.
476 https://doi.org/10.1016/j.memsci.2014.01.065.
477 Luo, J., Meyer, A. S., Jonsson, G., & Pinelo, M. (2013). Fouling-induced enzyme
478 immobilization for membrane reactors. *Bioresource Technology*, *147*, 260–268.
479 https://doi.org/10.1016/j.biortech.2013.08.019.
480 Luo, J., Meyer, A. S., Jonsson, G., & Pinelo, M. (2014b). Enzyme immobilization by fouling
481 in ultrafiltration membranes: Impact of membrane configuration and type on flux
482 behavior and biocatalytic conversion efficacy. *Biochemical Engineering Journal*, *83*,

79–89. https://doi.org/10.1016/j.bej.2013.12.007.

Luo, J., & Wan, Y. (2013). Effects of pH and salt on nanofiltration-a critical review. *Journal of Membrane Science*, *438*, 18–28. https://doi.org/10.1016/j.memsci.2013.03.029.

Martearena, M. R., Daz, M., & Ellenrieder, G. (2008). Synthesis of rutinosides and rutinose by reverse hydrolysis catalyzed by fungal α-L-rhamnosidases. *Biocatalysis and Biotransformation*, *26*(3), 177–185. https://doi.org/10.1080/10242420701568617.

Mishra, P., & Kar, R. (2003). Treatment of grapefruit juice for bitterness removal by Amberlite IR 120 and Amberlite IR 400 and alginate entrapped naringinase enzyme. *Journal of Food Science*, *68*(4), 1229–1233. https://doi.org/10.1111/j.1365-2621.2003.tb09630.x.

Norouzian, D., Hosseinzadeh, A., Inanlou, D. N., & Moazami, N. (2000). Production and partial purification of naringinase by *Penicillium decumbens* PTCC 5248. *World Journal of Microbiology and Biotechnology*, *16*, 471–473. https://doi.org/10.1023/A:1008962131271.

Olson, A. C., Gray, G. M., & Guadagni, D. G. (1979). Naringin bitterness of grapefruit juice debittered with naringinase immobilized in a hollow fiber. *Journal of Food Science*, *44*, 1358–1361. https://doi.org/10.1111/j.1365-2621.1979.tb06438.x.

Ono, M., Tosa, T., & Chibata, I. (1978). Preparation and properties of immobilized naringinase using tannin-aminohexyl cellulose. *Agricultural and Biological Chemistry*, *42*(10), 1847–1853. https://doi.org/10.1080/00021369.1978.10863264.

Prazeres, D. M. F., & Cabral, J. M. S. (1994). Enzymatic membrane bioreactors and their applications. *Enzyme and Microbial Technology*, *16*(9), 738–750. https://doi.org/10.1016/0141-0229(94)90030-2.

Ribeiro, I. A. C., & Ribeiro, M. H. L. (2008). Kinetic modelling of naringin hydrolysis using a bitter sweet alfa-rhamnopyranosidase immobilized in k-carrageenan. *Journal of Molecular Catalysis B: Enzymatic*, *51*(1–2), 10–18. https://doi.org/http://dx.doi.org/10.1016/j.molcatb.2007.09.023.

509 Rivero-Pérez, M. D., Muñiz, P., & González-Sanjosé, M. L. (2007). Antioxidant profile of red
510 wines evaluated by total antioxidant capacity, scavenger activity, and biomarkers of
511 oxidative stress methodologies. *Journal of Agricultural and Food Chemistry*, *55*(14),
512 5476–5483. https://doi.org/10.1021/jf070306q.
513 She, Q., Tang, C. Y., Wang, Y. N., & Zhang, Z. (2009). The role of hydrodynamic conditions
514 and solution chemistry on protein fouling during ultrafiltration. *Desalination*, *249*(3),
515 1079–1087. https://doi.org/10.1016/j.desal.2009.05.015.
516 Sigurdardóttir, S. B., Lehmann, J., Ovtar, S., Grivel, J. C., Negra, M. D., Kaiser, A., & Pinelo,
517 M. (2018). Enzyme immobilization on inorganic surfaces for membrane reactor
518 applications: Mass transfer challenges, enzyme leakage and reuse of materials.
519 *Advanced Synthesis and Catalysis*, *360*(14), 2578–2607.
520 https://doi.org/10.1002/adsc.201800307.
521 Sitanggang, A. B., Sumitra, J., & Budijanto, S. (2021). Continuous production of tempe-
522 based bioactive peptides using an automated enzymatic membrane reactor. *Innovative*
523 *Food Science and Emerging Technologies*, *68*, 102639.
524 https://doi.org/10.1016/j.ifset.2021.102639.
525 Soares, N. F. F., & Hotchkiss, J. H. (1998). Bitterness reduction in grapefruit juice through
526 active packaging. *Packaging Technology and Science*, *11*(1), 9–18.
527 https://doi.org/10.1002/(SICI)1099-1522(199802)11:1<9::AID-PTS413>3.0.CO;2-D.
528 Stinco, C. M., Fernández-Vázquez, R., Hernanz, D., Heredia, F. J., Meléndez-Martínez, A.
529 J., & Vicario, I. M. (2013). Industrial orange juice debittering: Impact on bioactive
530 compounds and nutritional value. *Journal of Food Engineering*, *116*(1), 155–161.
531 https://doi.org/10.1016/j.jfoodeng.2012.11.009.
532 Tsen, H. Y., Tsai, S. Y., & Yu, G. K. (1989). Fiber entrapment of naringinase from *Penicillium*
533 sp. and application to fruit juice debittering. *Journal of Fermentation and*
534 *Bioengineering*, *67*(3), 186–189. https://doi.org/https://doi.org/10.1016/0922-

338X(89)90120-7.

Wang, C. Y., Wang, Y. T., Wu, S. J., & Shyu, Y. T. (2018). Quality changes in high hydrostatic pressure and thermal pasteurized grapefruit juice during cold storage. *Journal of Food Science and Technology*, *55*(12), 5115–5122. https://doi.org/10.1007/s13197-018-3452-z.

Wang, Y. N., & Tang, C. Y. (2011). Protein fouling of nanofiltration, reverse osmosis, and ultrafiltration membranes-The role of hydrodynamic conditions, solution chemistry, and membrane properties. *Journal of Membrane Science*, *376*(1–2), 275–282. https://doi.org/10.1016/j.memsci.2011.04.036.

Yujun, W., Jian, X., Guangsheng, L., & Youyuan, D. (2008). Immobilization of lipase by ultrafiltration and cross-linking onto the polysulfone membrane surface. *Bioresource Technology*, *99*(7), 2299–2303. https://doi.org/10.1016/j.biortech.2007.05.014.

Zhang, Y. H., Ru, Y., Jiang, C., Yang, Q. M., Weng, H. F., & Xiao, A. F. (2020). Naringinase-catalyzed hydrolysis of naringin adsorbed on macroporous resin. *Process Biochemistry*, *93*(August 2019), 48–54. https://doi.org/10.1016/j.procbio.2020.03.014.

Zheng, Y., Zhang, W., Tang, B., Ding, J., Zheng, Y., & Zhang, Z. (2018). Membrane fouling mechanism of biofilm-membrane bioreactor (BF-MBR): Pore blocking model and membrane cleaning. *Bioresource Technology*, *250*(August 2017), 398–405. https://doi.org/10.1016/j.biortech.2017.11.036.

Zhu, X. Y., Chen, C., Chen, P. C., Gao, Q. L., Fang, F., Li, J., & Huang, X. J. (2016). High-performance enzymatic membrane bioreactor based on a radial gradient of pores in a PSF membrane via facile enzyme immobilization. *RSC Advances*, *6*(37), 30804–30812. https://doi.org/10.1039/c5ra25602j.

Figure Captions

Fig. 1. Permeate flux and filtration resistances during naringinase immobilization as a function of (A) membrane pore size and configuration, and (B) transmembrane pressure. Latin letters (a-c) indicate significant difference (p<0.05) between (A) different pore sizes or (B) transmembrane pressures for each resistance, Greek letters α-β indicate significant difference (p<0.05) between different configurations for each resistance**.** Immobilization conditions: (A) 0.2 MPa, 0.3 g L^{-1} of enzyme in acetate buffer at pH5; (B) Biomax 10, reverse mode, 0.2 g L^{-1} of enzyme in acetate buffer at pH5.

Fig. 2. Permeate flux and filtration resistances during naringinase immobilization as a function of (A) enzyme concentration and (B) immobilization pH. Latin letters (a-d) indicate significant difference (p<0.05) between (A) different enzyme concentrations or (B) pH for each resistance. Immobilization conditions: Biomax 10 reverse mode, 0.2 MPa; (A) acetate buffer pH5; (B) 0.3 g L^{-1} of enzyme.

Fig. 3. Effect of glutaraldehyde concentration on naringin conversion. Immobilization conditions: Biomax 10, reverse mode, 0.2 MPa, 0.3 g L^{-1} of enzyme in acetate buffer at pH5.

Fig. 4. (A) Naringin conversion and (B) permeate flux in the enzymatic membrane reactor with immobilized naringinase during the successive cycles of grapefruit treatment. Operating conditions: 50 ºC and 0.025 MPa.

Table 1

Effect of molecular weight cut-off and configuration of the membrane, and transmembrane pressure (TMP) on immobilization efficiency.[1]

Membrane*	Enzyme amount (mg)					IE (%)
	Feed	Permeate	Washing residue	Retentate	Loading	
Biomax 10-reverse mode	8.97 ± 0.22	not detected	not detected	1.14 ± 0.21	7.83 ± 0.16	$87.3 \pm 1.6^{b\beta}$
Biomax 30-reverse mode	8.82 ± 0.36	1.30 ± 0.19	not detected	1.18 ± 0.26	6.33 ± 0.32	71.8 ± 0.7^{a}
Biomax 10-normal mode	9.07 ± 0.14	not detected	not detected	7.55 ± 0.64	1.52 ± 0.60	$16.7 \pm 6.4^{\alpha}$
TMP (MPa)**						
0.1	6.02 ± 0.25	not detected	not detected	0.32 ± 0.00	5.71 ± 0.25	94.7 ± 0.2^{B}
0.2	6.06 ± 0.42	not detected	not detected	0.77 ± 0.26	5.11 ± 0.34	87.3 ± 3.5^{A}
0.3	5.79 ± 0.21	not detected	not detected	0.39 ± 0.01	5.39 ± 0.21	93.2 ± 0.3^{AB}

[1]IE= immobilization efficiency. Different lowercase Latin letters (a-b), Greek letters (α-β) or uppercase Latin letters (A-B), indicate significant difference ($p<0.05$) between different molecular weight cut-off, configurations, or pressures, respectively.

*Immobilization parameters: 0.2 MPa, 0.3 g L^{-1} of enzyme and acetate buffer at pH 5.

**Immobilization parameters: Biomax 10 in reverse mode, 0.2 g L^{-1} of enzyme and acetate buffer at pH 5.

Table 2

Effect of enzyme concentration and immobilization pH on immobilization efficiency (IE).[1]

[E] (g L^{-1})*	Enzyme amount (mg)					IE (%)
	Feed	Permeate	Washing residue	Retentate	Loading	
0.2	6.06 ± 0.42	not detected	not detected	0.77 ± 0.26	5.11 ± 0.34	87.3 ± 3.5[a]
0.3	8.97 ± 0.22	not detected	not detected	1.14 ± 0.21	7.83 ± 0.16	87.3 ± 1.6[a]
0.4	11.76 ± 0.30	not detected	not detected	1.74 ± 0.48	10.02 ± 0.59	85.2 ± 3.4[a]
pH**						
3	8.81 ± 0.27	not detected	not detected	0.60 ± 0.12	8.22 ± 0.19	93.3 ± 0.9[B]
5	8.80 ± 0.15	not detected	not detected	0.67 ± 0.01	8.13 ± 0.15	92.3 ± 0.1[B]
6	8.86 ± 0.47	0.15 ± 0.04	0.95 ± 0.35	0.65 ± 0.22	7.12 ± 0.24	80.4 ± 4.5[A]

[1]IE= immobilization efficiency; ND= not detected. Different lowercase letters (a-b) or uppercase letters (A-B) indicate significant difference (p<0.05) between different enzyme concentrations or pH, respectively.

*Immobilization parameters: Biomax 10 in reverse mode, 0.2 MPa and acetate buffer at pH 5.

**Immobilization parameters: Biomax 10 in reverse mode, 0.2 MPa and 0.3 g L^{-1} of enzyme in citrate phosphate buffer.

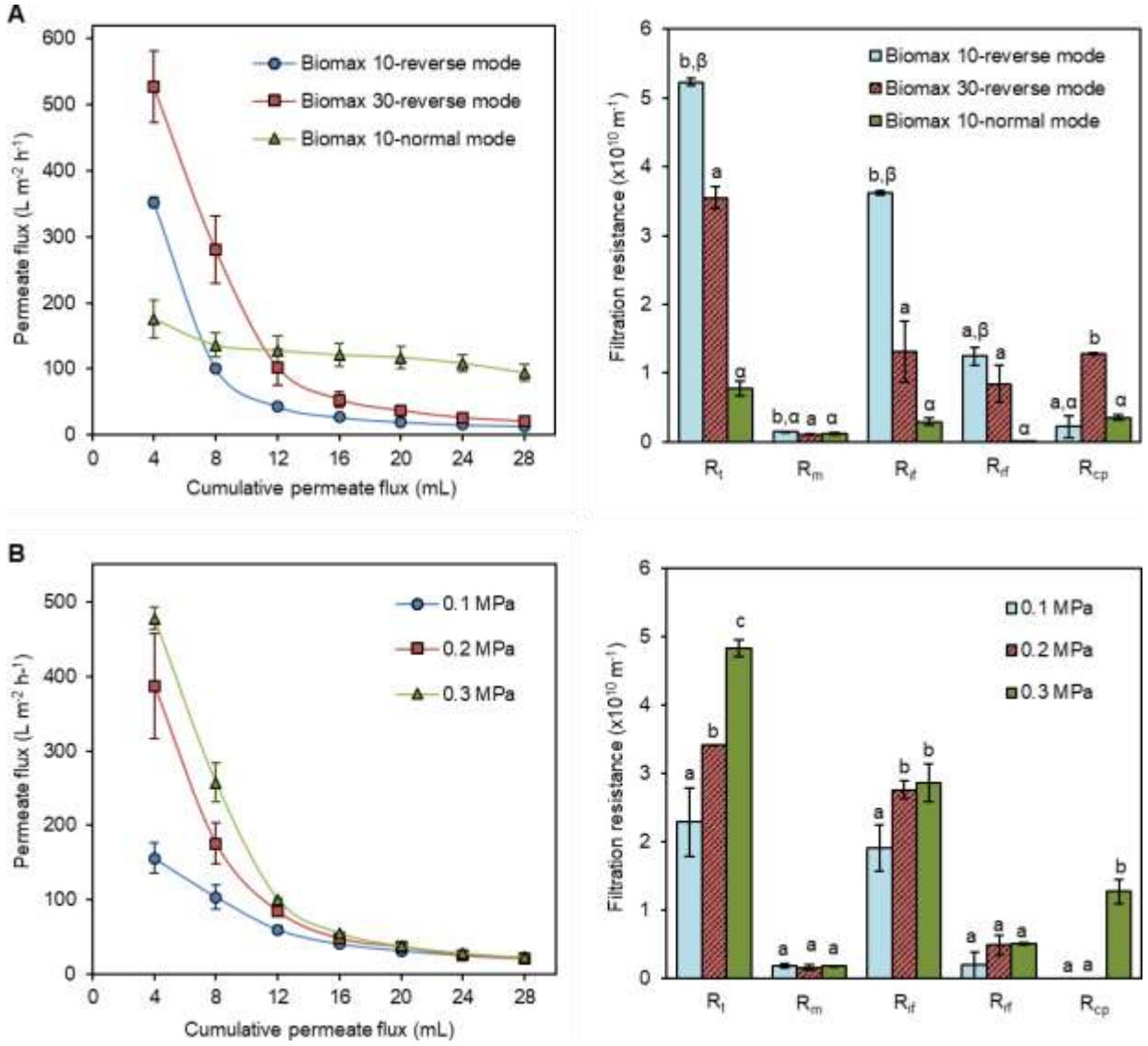

Fig. 1. Permeate flux and filtration resistances during naringinase immobilization as a function of (A) membrane pore size and configuration, and (B) transmembrane pressure. Latin letters (a-c) indicate significant difference (p<0.05) between (A) different pore sizes or (B) transmembrane pressures for each resistance, Greek letters α-β indicate significant difference (p<0.05) between different configurations for each resistance**.** Immobilization conditions: (A) 0.2 MPa, 0.3 g L^{-1} of enzyme in acetate buffer at pH5; (B) Biomax 10, reverse mode, 0.2 g L^{-1} of enzyme in acetate buffer at pH5.

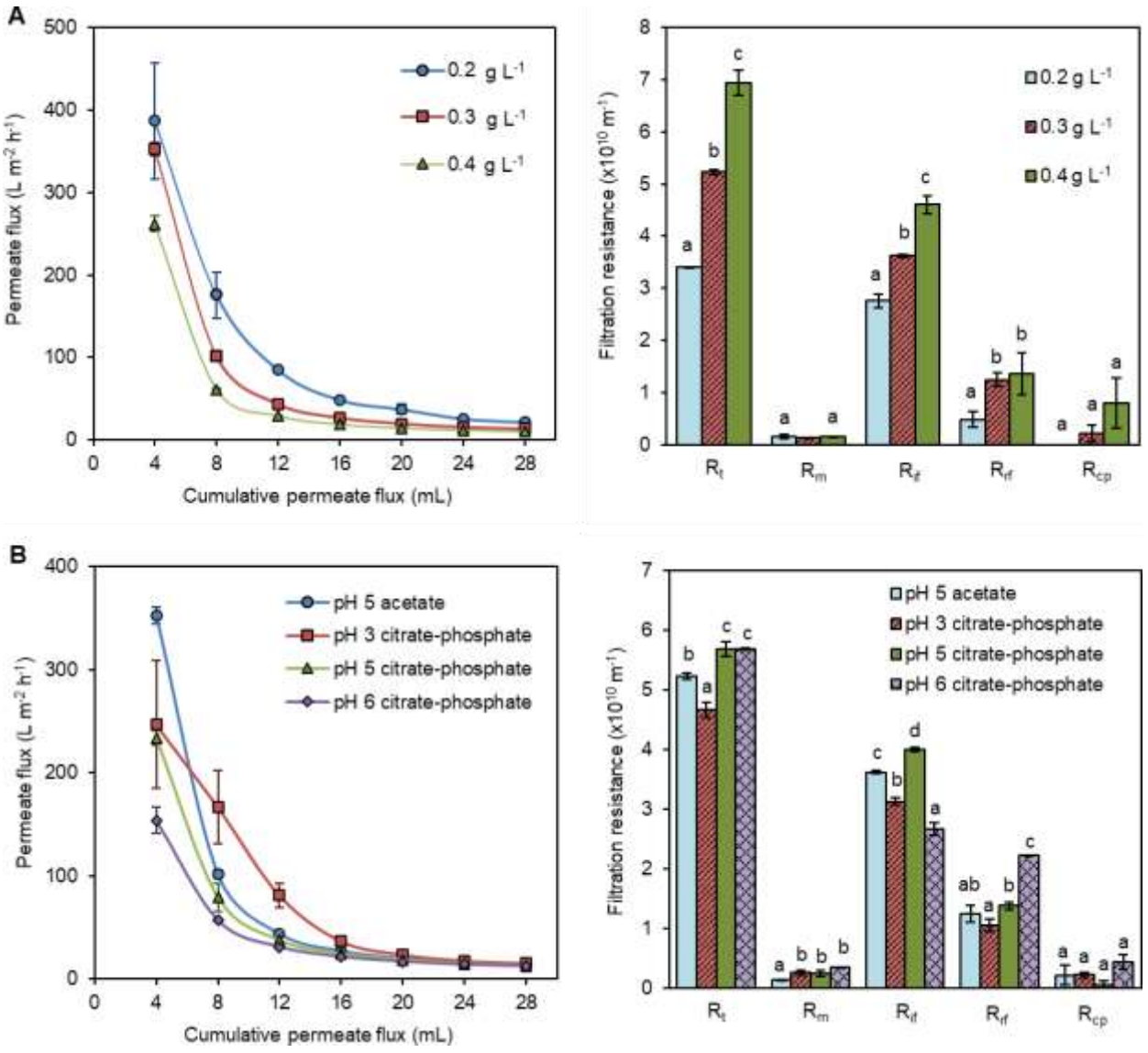

Fig. 2. Permeate flux and filtration resistances during naringinase immobilization as a function of (A) enzyme concentration and (B) immobilization pH. Latin letters (a-d) indicate significant difference (p<0.05) between (A) different enzyme concentrations or (B) pH for each resistance. Immobilization conditions: Biomax 10 reverse mode, 0.2 MPa; (A) acetate buffer pH5; (B) 0.3 g L^{-1} of enzyme.

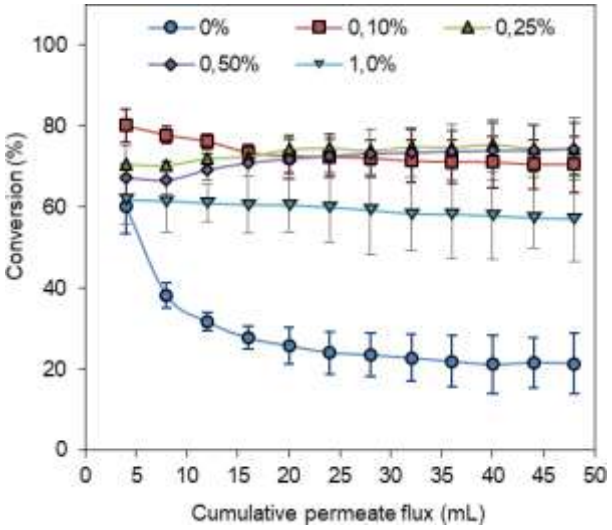

Fig. 3. Effect of glutaraldehyde concentration on naringin conversion. Immobilization conditions: Biomax 10, reverse mode, 0.2 MPa, 0.3 g L^{-1} of enzyme in acetate buffer at pH5.

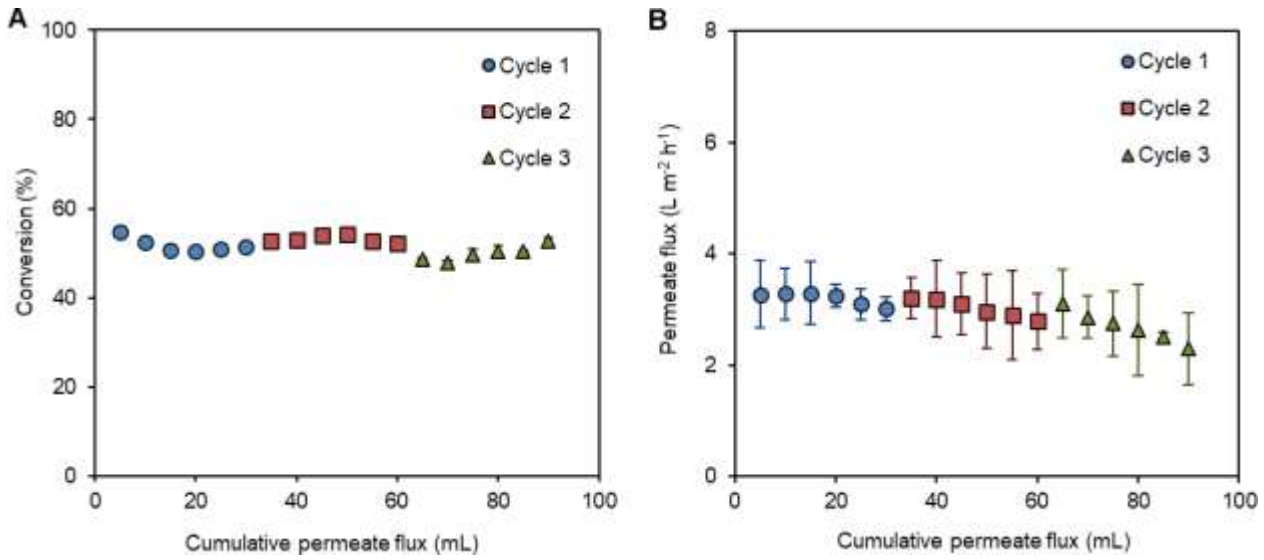

Fig. 4. (A) Naringin conversion and (B) permeate flux in the enzymatic membrane reactor with immobilized naringinase during the successive cycles of grapefruit treatment. Operating conditions: 50 ºC and 0.025 MPa.